INVESTIGATION OF NEAR FIELD INDUCTIVE COMMUNICATION SYSTEM MODELS, CHANNELS AND EXPERIMENTS

Johnson I. Agbinya*

Department of Electronic Engineering, La Trobe University, Bundoora, Melbourne, Australia

Abstract—Near-field inductive channels created between two or more magnetically coupled inductive nodes are studied in this paper. Peer-to-peer configurations and array architectures are discussed. The array channels are used for cooperative relaying with inductive methods with potential to provide range extension and enhanced data rate access in magnetic induction communication systems. The received power shows the presence of the nearest neighbour interactions and the influences of higher order coupling from nodes two or more positions away from the receiver. This influence causes phase changes in the communication system. Four methods of exciting the antenna arrays are proposed. These are array edge excitation, center excitation, collinear array excitation and multi-array excitation. Experiments with hardware nodes show that while array edge excitation provides increased power at the array edge, it is out performed by array center excitation which results to twice the power captured at the array center node compared to the power captured at edge excited first element. We demonstrate by example that a receiver is influenced most by its neighbouring nodes on both sides and that the effects of second and third tier neighbours are relatively insignificant.

1. INTRODUCTION

Electromagnetic (EM) waves have traditionally played the leading role in most telecommunication systems and applications. Both the electric and magnetic fields of an EM wave propagate together as the Poynting vector with the two vectors oriented at ninety degrees to each other. Near an antenna in its near-field region the magnetic field is the

* Corresponding author: Johnson Ihyeh Agbinya (j.agbinya@latrobe.edu.au).

dominant component while far away from the antenna in the far-field region, the electric field becomes dominant. The magnetic field energy in the near-field can be acquired through mutual coupling of inductors. The power in the magnetic field decays very fast in the channel as an inverse sixth power of distance while the electric field decays as an inverse quadratic function of distance. In the far-field region of an antenna therefore, most of the energy in an EM wave is held in the electric field.

Environmental conditions make the use of such EM waves not suitable for communications underground (mines, tunnels, oil and gas wells) and in water. This is because of the intrinsic properties (permittivity and permeability) of these media. First in underground communications EM waves encounter at least three major problems of high path loss, rapid changes in the channel conditions due to the changing nature of the terrain (water and soils of varying EM attenuation regimes) and need large antennas. Under these conditions, terrestrial EM communications do not perform optimally [1–4]. Changing soil characteristics with temperature and water content causes large bit error rates and degrades performance. Second communication in coastal regions also face changing conditions due to the dynamic environmental factors such as shallow bathymetry, wave and tidal action, acoustically reflective boundaries and marine growth. In coastal regions, reflectivity, noise and multipath effects render conventional radio and acoustical systems significantly ineffective. The signal degradation sources make both acoustic and EM navigation and communication systems unreliable [5]. However many ecological and industrial navigation situations occur in coastal regions and many of the mine warfare operations are performed in such environments. Third short range communication networks such as body area networks encounter large bio-impedances contributed by biological tissues which for safety reasons negate extended use of EM waves for communications and power transcutaneous power transfer. Hence a physical access technology is required which help to limit and/or solve some of the problems associated with the above terrains.

2. RELATED WORK

Magnetic induction (MI) communication is a promising alternative physical access method to EM waves first in terms of its ability to create a so-called secure communication 'bubble' [6, 7] around a transmitter. Second, it solves some or all of the problems associated with EM communications. In EM radio communications, the radiation resistance of a conventional antenna system must be made fairly

higher than the ground losses to ensure that strong electric field is produced. In MI communication however, the radiation resistance of the antenna coils are very small and insignificant EM waves created do not propagate far. Rather a magnetic field is created by the transmitter which induces a sympathetic flux in the receiver coil. The sympathetic receiver flux is proportional to the current in the transmitter loop and the inductances of the transmitter and receiver loops. The role of the channel appears as gain reduction in the receiver power (the so-called coupling coefficient) and has a dramatic attenuating impact on the received power at long distances. The near absence of the EM field means that the magnetic field does not propagate, is quasi-static in air and in most medium it is primarily diffusive. Furthermore, the associated very low power applications means they are relatively safe and have less impact on biological tissues with little to no heating effects. Hence they are popular in implantable hearing aids and magnetic resonance imaging (MRI) systems. As a result the application of magnetic fields in medicine dates back to hundreds of years [22]. Near-Field Magnetic Induction Communication (NFMIC) is a wireless form of short range communication, up to 5 m, using near field magnetic flux for data transmission [11, 12]. In reality they operate as proximity communication systems. They are an efficient means of creating secure self-powered body area networks, payment cards, biomedical monitoring, near field mobile phones, MP3 players, body implants and many more [6, 9, 10].

Compared to other short range communication technologies such as *Bluetooth,* MI is about six times more power efficient. Moreover, it promotes frequency reuse over short and long distances. It also contributes less interference with other existing radio frequency (RF) communication systems, because it does not have to operate in busy 2.45 GHz region and the data needs to be communicated within a person's NFMIC '*bubble*' [1]. A major advantage of MIC over traditional EM RF-based systems is that the MI waves are not generally affected by the environment. Therefore, this characteristic of near field magnetic induction communication makes it considerably advantageous over EM RF-based communication systems in applications such as underground or underwater communications. However, the impact of path loss (a function of distance to power of 6) is critical in NFMIC compared to RF networks. Therefore, NFMIC targets the medium capacity personal area networks with close proximity.

A MI communication system was recently demonstrated in [6, 13, 14, 23] for underground communication in mines where the effects of the terrain and the environment strongly reduce the perfor-

mance of RF methods but it led to poor range coverage a feature that is suited to secure short range 'communication in a bubble'. Therefore, in the application in [2] a magneto-inductive waveguide was used to extend the range of communications. In a magneto-inductive waveguide there is no need for the relay coils to be individually powered since each coil induces flux to its neighbors and through that means information is carried from neighbor to neighbor until the receiver is reached. Magnetic waveguides were studied by Shamonina and Solymar [15–17]. They showed that with proper terminations power losses are minimized in the waveguide system. The impedance matching at the receiver blocks backward waves and only forward magneto-inductive waves exist in the system. If discontinuities exist in the waveguide system, reflections are observed causing reduced power coupling to the load. Discontinuities in MI waveguides occur when the impedances of neighbouring coils are different. Hence in this paper non-reflective waveguides are assumed by making the links identical or using identical coils at each node.

The application of MI techniques in remote wireless power transfer has also been studied recently in [8, 18] and the energy scavenging properties reported by Jiang et al. [19, 20]. The authors evaluated the effects of small loads and large loads from the communication range point of view. Understandably, coupled power to the receiver load is proportional to the load and hence it is expected that smaller range would be obtained when the parasitic resistances of the coils are large. Recently we studied the MI communication bubble created by an MI peer-to-peer system [6, 23] as basis for MI transceiver design. It was shown that the size of the bubble is determined by the quality factors (Q), the efficiencies (η) and the coupling coefficient ($k(x)$) between the coils. We established the basis for understanding the nature and size of the MI bubble. A MI bubble is defined as the sphere of communication around the inductive loop operating in the near-field region. Outside the bubble it is assumed that the flux created by the loop is nearly zero. Outside the bubble however, the loop has remnant EM waves and behaves as RF antenna marginally. The objective in MI system design is to ensure that the vanishingly small waves are not detectable outside the bubble and if there is to provide a means of limiting it. The need to couple power efficiently to the receiver is however paramount in MI systems.

Based on work by Agbinya and Masihpour in [24], Fatiha et al. [25] recently characterized the magnetic link performance of an embedded ingestible capsule at 40 MHz with the objective of determining the efficiency of magnetic systems. Also a recent brief discussion on inductive channel is given by Lee in [26]. Inductive

channels and link budget, therefore, remain an active area of current interest. In this paper we provide a models and thorough analysis of magnetic links and channels with the objective of helping to establish more efficient inductive communication under different conditions and system configurations.

In the rest of the paper we discuss the general principles of inductive communications in Section 3. Inductive communication channels are introduced in Section 4 from the waveguide model point of view and a thorough analysis of the peer-to-peer inductive link is provided. To allow the link performances to be assessed, Section 5 provides various techniques for exciting the magnetic communication system and elaborate expressions for the received power at various positions along the chain of nodes are provided. Simulations of the effects of nearest neighbor interaction on array performance are given in Sections 6 with conclusions drawn in the Section 7.

3. PRINCIPLES OF MAGNETIC INDUCTION COMMUNICATIONS

In magnetic communications, the MI transmitter uses typically a resonant small coil of small radius and a similar resonating coil acting as the receiver (Figure 1) [27]. The transmitter is modeled as a magnetic dipole operating at very low frequencies and hence any electric field created is vanishingly small and has no far field effects and hence cannot be detected in the far field region and hence suited to clandestine operations. The magnetic moment m $(m = N \cdot I \cdot A)$ created on axis in an air core system is proportional to the number of turns N of the antenna coil, the area A (m^2) of the coil and the current I (amperes) flowing through it. The magnetic moment can be increased by deploying the coil on a magnetically permeable core such as a ferrite rod so that $m = \mu_r N \cdot I \cdot A$, where $\mu_r > 1$ is the relative permeability of the core material and is a strong function of the orientation of the coil.

Communication using magnetic field requires that the flux be modulated and many of the conventional modulation schemes may
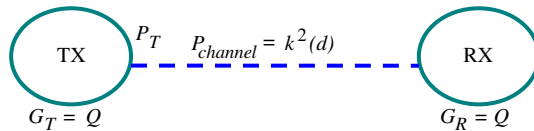
Figure 1. Peer-to-peer MI communication system.

be employed depending on the application [1, 23]. The voltage which can be induced in the receiver coil is proportional to the magnetic flux density, the area of the coil, the operating frequency and the number of turns of the coil. This voltage can also be enhanced by laying the coil on a magnetically permeable material with permeability μ_x. The induced voltage is

$$V = \mu_x 2\pi B \cdot NA \cdot f \tag{1}$$

By tuning the receiver coil to resonate with the transmitter, further enhancement of the induced voltage is obtained. Furthermore, by using a coil of higher Q and higher coil efficiency η, this voltage can also be increased while sacrificing bandwidth [2, 6, 23]. The magnetic field strength developed by the transmitter decays at a rate proportional to the inverse d to power three $(1/d^3)$ and hence the power decay is proportional to $(1/d^6)$. MI bubble factors were recently proposed in [6]. While most authors assume that the size of the near field magnetic induction (NFMI) bubble is the same as the edge of near field in [6] we have demonstrated that the two are not the same. The signal level at the near field edge is still too high and easily available for interception with a sensitive instrument and [6] quantifies the bubble for that purpose. Intuitively, we define the magnetic bubble in terms of the sensitivity of the receiver [6]. The power transferred to a receiver load resistance R_L is proportional to the transmitted power, the quality factors of the coils, the coupling coefficients and their efficiencies [6]. When the radius of the transmitting coil is smaller than the communication range $(r_1 \ll x)$ the received power at resonance at location x is [6]:

$$\begin{aligned} P_r(\omega = \omega_0) &= P_t Q_1 Q_2 \eta_1 \eta_2 k^2(x) \\ &= P_t Q_1 Q_2 \eta_1 \eta_2 \frac{r_1^3 r_2^3}{\left(x^2 + r_1^2\right)^3} \cong \frac{\sigma}{x^6}; \qquad r_1 \ll x \end{aligned} \tag{2}$$

where $\sigma = P_t Q_1 Q_2 \eta_1 \eta_2 r_1^3 r_2^3$. The received power is therefore, a decreasing function of distance to power six (6). The factor σ was defined in [6] as the *distance bubble factor* and quantifies the communication range to within a short radius centered on the transmitter which is traditionally called the "bubble". Although the bubble range is a function of the quality factors and coil efficiencies it is typically a couple of meters and a few centimeters for embedded medical devices. The fast power decay is considerably significant for secure communications where the objectives are the security of the transmitter and data and the safety of the person carrying the transceiver. The capacity of such a system was recently given by the authors in [6, 23] and in [10]. Let d be the distance at which the received

signal power is equal to the sensitivity of the receiver $P_r = P_S$, where P_S is the sensitivity of the receiver. This indicates that the size of the bubble is not fixed but rather is a function of the receiver sensitivity. We may also define the size of the bubble in terms of the signal to noise ratio (SNR) of the system and defines the radius of the magnetic bubble as the distance where the received signal power is equal to the noise power ($P_r = N$ or SNR $= 1$). Therefore, the system capacity at the edge of the NFMI bubble is

$$C = B_f f_0 \log_2 \left(1 + \frac{P_{rd}\,(\omega = \omega_0)}{N} \right) = B_f f_0 \log_2 2 = B_f f_0 \qquad (3)$$

At the edge of the bubble, no signal amplification helps as noise is also amplified equally so the bubble remains secure from someone outside it. Bear in mind that the $3\,\mathrm{dB}$ fractional bandwidth B is defined purely by the Q of the coils and the centre frequency [10], where

$$B_f = \frac{B}{f_0} = \begin{cases} \frac{1}{Q_1}; & \text{if } Q_1 > Q_2 \\ \frac{1}{Q_2}; & \text{if } Q_2 > Q_1 \end{cases} \qquad (4)$$

Thus for large capacity, the bandwidth of the system must be large. However, unlike inductive wireless power transfer that requires large Q, inductive communication systems are favoured by small quality factors so as to maximize B_f. By letting $Q_1 = Q_2 = Q$ in Equation (4), this expression reduces to $B_f = 1/Q$ and the capacity at the edge of the bubble (assuming the SNR $= 1$ there)

$$C = B_f f_0 = f_0/Q \qquad (5)$$

is determined exclusively by the Q-factors of the coils and the resonance centre frequency. For a resonance frequency in the ISM band of $13.56\,\mathrm{MHz}$ and $Q = 40$, this capacity is approximately $339\,\mathrm{kbps}$. The capacity at the edge of the bubble is directly proportional to the resonant frequency. The higher Q is, the lower the capacity at the edge of the bubble. This paradox is the major benefit of NFMI. The performance should, therefore, be evaluated in terms of the efficiency of the communication bubble. A typical magnetic induction device draws as low current as $7\,\mathrm{mA}$ to transfer voice or data over a couple of meters. To their advantage magnetic induction communication systems are not generally affected by the environment. From the MI power equation the effect of the environment is given by the permeability of the materials in the link and source (sink). The permeability of the medium can be used to advantage to amplify the signal power in the link. Thus paramagnetic and ferromagnetic channels will strengthen the magnetic field from the transmitter to the receiver.

Fading, multipath propagation, interference and noise which plague electromagnetic (EM) systems are not problems in MI systems

but rather one of the main problems is how to improve upon the rapid decline in MI power due to the inverse sixth power decay with range. Current literature is devoid of the performance evaluation of MI technology from a commercial hardware point of view. Recently FreeLinc [7] marketed MI radios of very short range typically around 1.5 m.

4. MI COMMUNICATION CHANNELS

The Section 3 describes simple peer-to-peer systems. Similar work is reported in [2] by Sun and Akyildiz. Figure 2 shows the general framework for magnetic waveguides as a chain of resonant loops [16, 17, 21]. The source loop transmits information and this is relayed by the relaying nodes until the signal reaches the receiver. We now show that the model in [2] is similar to the Agbinya-Masihpour model [6, 23] if a common framework is used to compare them by establishing a common formalism. The common formalism defines the following parameters. The efficiencies of the coils are:

$$\eta = R_S/R_S + R_L \cong 1 \quad \text{or} \quad R_S \gg R_L \tag{6a}$$

In Figure 2 for convenience we have combined the resistances as $R_R = R_S + R_L$. The quality factors at the transmitter and receiver are

$$Q_T = \omega L_T/R_{LT} \quad \text{and} \quad Q_R = \omega L_R/R_{LR} \tag{6b}$$
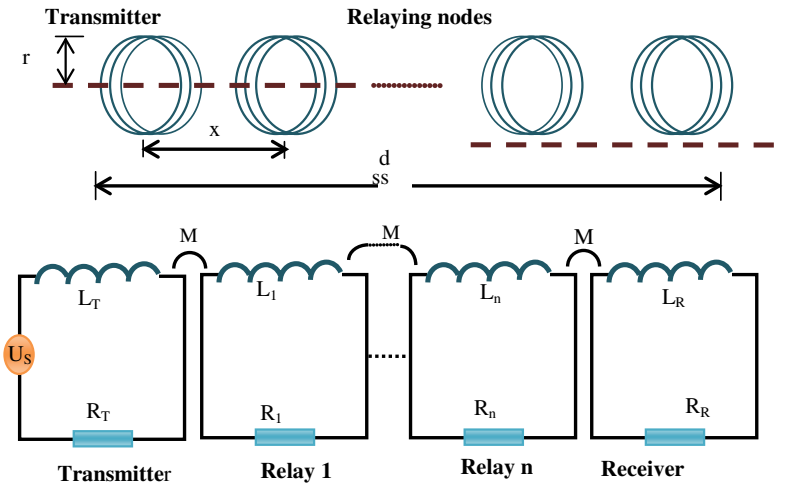
Figure 2. Magnetic waveguide and circuit model.

The self resistances of the transmitter and receiver coils of radius r are usually very small and given as $R_{LT} = R_t = 2\pi \cdot r_T N_T R_0$ and $R_{LR} = R_r = 2\pi \cdot r_R N_R R_0$ respectively.

By substituting these in Equation (6b) when the length $l = 2\pi \cdot r \cdot N \gg 0.9r$, $N_T = N_R = N$, then

$$L = \mu A \cdot N^2/(l + 0.9r);$$

$$\text{then} \qquad L_T \approx 0.5\mu r_T \cdot N_T \quad \text{and} \quad L_R \approx 0.5\mu \cdot r_R \cdot N_R \qquad (6c)$$

Therefore, when the quality factors of the transmitter and receiver are equal we have shown in [1] that the coupling coefficient also is.

$$k^2(d) = \frac{\mu^2 A_R^2 \cdot r_T^4}{4 \cdot L_T L_R \left(d^2 + r_T^2\right)^3} = \frac{\pi^2 r_T^3 r_R^3}{N_T N_R d^6} \qquad (6d)$$

$Q_T = \omega\mu/4\pi \cdot R_{0T}$ and $Q_R = \omega\mu/4\pi \cdot R_{0R}$. Therefore, the received power is

$$P_R = P_T Q_T Q_R \eta_T \eta_R k^2(d) = P_T Q^2 k^2(d) \qquad (7)$$

This equation models two inductive antennas with gain Q and path loss given by $k^2(d)$ as shown in the Figure 1. This figure is fundamental for the peer-to-peer MI nodes systems in general. This common formalism allows us to re-write the model of Equation (2) when we set $\eta_1 = \eta_2 = 1$. Therefore, the traditional Agbinya model (AM) [1, 23] can be written as:

$$P_R = \frac{\omega^2 \mu^2}{16\pi^2 R_0^2} \cdot \frac{r_T^3 r_R^3 \pi^2 P_T}{N_T N_R d^6} = \frac{\omega^2 \mu^2 r_T^3 r_R^3 P_T}{16 R_0^2 N_T N_R d^6} = Q^2 k^2(d) P_T \qquad (8)$$

4.1. Magnetic Waveguide Link: Model 1

To compare the model in [1] with the model in [2], we derive the link budgets for both using the received power in the standard case defined as

$$\frac{P_R}{P_T} = \frac{\omega\mu \cdot N_R r_T^3 r_R^3}{16 R_0 d^6} = \frac{\omega\mu}{4\pi R_0} \frac{\omega\mu}{4\pi R_0} \frac{\pi^2 r_T^3 r_R^3}{N_T N_R d^6} \frac{N_T N_R^2}{\omega\mu}$$

$$= \left(\frac{N_T N_R^2}{\omega\mu}\right) Q^2 k^2(d) \qquad (9)$$

The link budget equations for the two cases become: ($d = 10^\beta$ where for the AM case the link budget Equations (10) and (11))

$$\beta_{AM} = \frac{\{\mathbf{P}_T(\text{dBm}) - P_R(\text{dBm}) + 20 \cdot \log\mu + 20 \cdot \log\omega + 30\log(\mathbf{r}_{T}\mathbf{r}_{R})}{-[10 \cdot \log 16 + 20 \cdot \log R_0 + 10 \cdot \log N_T N_R]\}}{60} \qquad (10)$$

$$d_{AM} = 10^{\frac{P_T\,(dBm)-\mathbf{P}_R\,(dBm)+20\cdot\log\omega+30\log(\mathbf{r_T r}R)}{60}}$$
$$\times 10^{\frac{20\cdot\log\mu-10\cdot\log 16-20\cdot\log R_0-10\cdot\log N_T N_R}{60}} \tag{11}$$

The major limitation of MI communication is its rapid power decay and thus short range typically a couple of meters from the transmitter and therefore, unsuitable for applications such as wireless local area networks at larger range. Magneto-inductive waveguides have recently emerged as a method of extending the range of MI communications systems. We therefore propose a link budget for n section MI waveguide. Sojdehei et al. [5], Syms et al. [15], Shamonina [16], and Kalinin et al. [17] have established some of the theories for the MI waveguide used in this section. A peer-to-peer 'waveguide' is well analyzed and discussed by Agbinya et al. in [2, 6, 23]. Consider also the model in [2] based on our proposed framework in this paper. In doing so, we insert the defining equations in the framework in Equations 6(a)–(d). The ratio of the received power to the transmitted power is given by the expression [1, 2]:

$$\frac{P_R}{P_T} \approx \frac{\omega^2\mu^2 N_T N_R r_T^3 r_R^3 \sin^2\alpha}{8d^6} \cdot \frac{1}{4R_0\left(2R_0+\frac{1}{2}j\omega\mu N_T\right)} \tag{12}$$

In this equation, R_0 is the per unit resistance of the coils. All the other variables retain their usual meaning and the angle $\sin(\alpha)$ originates from integration of the magnetic potential of a magnetic dipole in Equation (6) in [2]. By assuming a low resistance loop, high signal frequency and large number of turns in the transmitter and receiver circuits $(R_0 \ll \omega\mu N_T)$ [2] the power ratio reduces to:

$$\frac{P_R}{P_T} \approx \frac{\omega\mu N_R r_T^3 r_R^3 \sin^2\alpha}{16R_0 d^6} \tag{13}$$

This model supports only peer-to-peer communication and does not deliver maximum power to the receiver load due to lack of resonance between the receiver and transmitter. For range extension and maximum power transfer, resonant relays with inductive waveguide are employed.

A MI waveguide consists of n sections which relay data as in Figure 2. The transmitter couples energy to the first coil near it and that coil couples energy to coil on its right and this process repeats until the receiver is reached. Thus the link Model 1 and range expression

are derived from the channel model equation in [2] and are:

$$\beta_{M1} = \frac{p_T\,(\text{dBm}) - P_R\,(\text{dBm}) + 10 \cdot \log \mu + 10 \cdot \log N_R}{60}$$
$$\times \left[\frac{30 \log (r_T\, r_R) - 10 \cdot \log 16 - 20 \cdot \log R_0}{60} \right] \quad (14)$$

The communication range is

$$d_{M1} = 10^{\frac{p_T\,(\text{dBm}) - P_R\,(\text{dBm}) + 10 \cdot \log \mu + 10 \cdot \log N_R}{60}}$$
$$\times 10^{\frac{+30 \log \left(r_T\, r_R \right) - 10 \cdot \log 16 - 20 \cdot \log R_0}{60}} \quad (15)$$

In the simulations to follow we use $r_T = 2.5\,\text{cm}$, $r_R = 1.5\,\text{cm}$, $N_T = N_R = 10$ and $R_0 = 0.0216\,\Omega/\text{cm}$. The communication distance is $0 \le d \le 6\,\text{m}$ and the frequencies are 13.56 MHz, 300 MHz and 900 MHz. The ratio of the received powers for the two models is

$$\frac{P_{R,AM}}{P_{R,M1}} = \frac{\omega \mu}{N_R^2 N_T R_0} \quad (16)$$

4.2. Magnetic Waveguide Link: Model 2

MI waveguide can be efficient in underground wireless communication systems if each magnetic coil is used as a relaying node for sending data without power consumption; by connecting a capacitor to each loop, maximum power is transferred at resonance. With this a path loss model is proposed and relates the transmitted power and the received power to the system parameters (permeability, per unit resistance of the wire of the transmitter and receiver coils, number of turns, their radii, transmitting frequency and communication range as given in [3]).

At resonance the impedance of each loop is resistive and the resonance frequency is $\omega_0 = 1 \big/ \sqrt{LC}$ and $\omega^2 = 1/LC$. This allows the value of the capacitor required for resonance at each relaying node to be determined for an inductor of radius 'a' as

$$C = \frac{2}{\omega^2 N^2 \mu \cdot \pi \cdot a} \quad (17)$$

Therefore, when the capacitor is in circuit, the path loss expression in a magnetic waveguide is:

$$\frac{P_R}{P_T} = \frac{\omega^2 N^2 \mu^2 r_T^3 r_R^3}{4x^6 2R_0 \left(4R_0 + \frac{\omega^2 N^2 \mu^2 r_T^3 r_R^3}{4x^6 2R_0} \right)} \times \left[j \left[\frac{4R_0}{\omega \mu N} \left(\frac{x}{a} \right)^3 + \frac{\omega \mu N}{4R_0} \left(\frac{a}{x} \right)^3 \right]^{-1} \right]^{2n} \quad (18)$$

The variable x is the separation between any two sections of the MI waveguide. Thus the total communication range d is divided into $n+1$

sections of length x, or $d/x = (n+1)$. The imaginary term dissolves to a real value because of the exponent $2n$ in Equation (18). The path loss is a real positive number for even n and for odd values of n has a negative value. Thus when the traditional magneto-inductive wave is present a positive value is obtained. A negative value indicates the presence of an evanescent wave with sign changes [21]. To illustrate the behavior of the MI waveguide the path loss expression is simplified into the so-called AM2 link budget and provides insight into the achievable range. By using the expressions for the Q factors, we rewrite the path loss equation as a product of two terms:

$$\frac{P_R}{P_T} = P_1 P_{2n} \tag{19}$$

$$P_1 = \frac{\omega^2 N^2 \mu^2 r_T^3 r_R^3}{4x^6 2R_0 \left(4R_0 + \frac{\omega^2 N^2 \mu^2 r_T^3 r_R^3}{4x^6 2R_0}\right)}$$

$$= \frac{\omega\mu}{4\pi R_0} \cdot \frac{\omega\mu}{4\pi R_0} \cdot \frac{N^2 \pi^2 k^2 (x)}{\left(2 + \frac{\omega\mu}{4\pi R_0} \cdot \frac{\omega\mu}{4\pi R_0} \cdot N^2 \pi^2 k^2 (x)\right)} \tag{20a}$$

$$P_1 = \frac{Q_T \cdot Q_R N^2 \pi^2 k^2 (x)}{(2 + Q_T \cdot Q_R \cdot N^2 \pi^2 k^2 (x))} \tag{20b}$$

By approximating $k^2 (x) \approx \frac{r_T^3 r_R^3}{x^6}$ (similar to neglecting Δd in the AM model), the second term is:

$$P_{2n} = \left[j \left[\frac{4R_0}{\omega\mu N} \left(\frac{x}{a}\right)^3 + \frac{\omega\mu N}{4R_0} \left(\frac{a}{x}\right)^3 \right]^{-1} \right]^{2n}$$

$$= \left(Q_T \cdot Q_R N^2 \pi^2 k^2(x)\right)^n \left[j \left(1 + \frac{\omega^2 \mu^2 N^2 \pi^2}{(4R_0\pi)(4R_0\pi)} k^2(x)\right)^{-1} \right]^{2n} \tag{21a}$$

Therefore

$$P_{2n} = \left(Q_T \cdot Q_R N^2 \pi^2 k^2 (x)\right)^n \left[\frac{j}{(1 + Q_T \cdot Q_R N^2 \pi^2 k^2 (x))} \right]^{2n} \tag{21b}$$

Therefore, the path loss equation becomes

$$\frac{P_R}{P_T} = \frac{Q_T \cdot Q_R N^2 \pi^2 k^2 (x)}{(2 + Q_T \cdot Q_R \cdot N^2 \pi^2 k^2 (x))} \left(Q_T \cdot Q_R N^2 \pi^2 k^2 (x)\right)^n$$

$$\times \left[\frac{j}{(1 + Q_T \cdot Q_R N^2 \pi^2 k^2 (x))} \right]^{2n} \tag{22}$$

Define $\beta = Q_T Q_R N^2 \pi^2 k^2(x)$ as the section path loss. The waveguide path loss is, therefore, given by the expression:

$$\frac{P_R}{P_T} = \frac{\beta \cdot \beta^n}{(2+\beta)} \left[\frac{j}{(1+\beta)} \right]^{2n} = \left(\frac{\beta^{n+1}}{(2+\beta)} \right) \left(\frac{1}{(1+\beta)} \right)^{2n} e^{j\pi n} \quad (23)$$

The phase term in Equation (23) accounts for the presence of two types of waves in the waveguide the traditional magneto-inductive wave and an evanescent wave whose modulus decays exponentially and changes signs between adjacent elements [21]. Syms et al. [21] have also explained the presence of higher-order interactions on the traditional MI wave causing the phase change and negative amplitude for odd n. For weak coupling between the coils, $k^2(x) \ll 1$, $\beta \ll 1$ and noting that $\exp(j\pi n) = \pm 1$ the above expression simplifies to

$$\frac{P_R}{P_T} = \frac{\beta^{n+1}}{2} \quad (24)$$

In this situation, the flux developed by the transmitter is weakly linked to the receiver coil and the overall waveguide power is a geometric product of the section path losses. For strong coupling between the coils $k^2(x) \approx 1$, and $\beta \gg 2$ and the expression reduces to:

$$\frac{P_R}{P_T} = \frac{\beta^n}{2} \left[\frac{j}{\beta} \right]^{2n} \quad (25)$$

For $n = 0$ we have the simple peer-to-peer MI system path loss equation. When $r_T = r_R = x$, we have $k(x) = 1$. The coupling coefficient cannot be more than unity or $r_T \cdot r_R$ cannot be greater than the section length (usually $r_T \cdot r_R \leq x^2$). The inequality $r_T \cdot r_R > x^2$ is an impossible situation as it is not possible that the receiver collects more flux than all the flux created by the transmitter. For $n = 0$ and β is unity the received power is a third of the transmitted power and we have the same result as in [2]:

$$\frac{P_R}{P_T} = \frac{1}{3} \left(\frac{1}{2} \right)^{2n} \quad (26)$$

This means that $\beta = Q_T Q_R N^2 \pi^2 k^2(x)$ or the equation required for determining optimum power transfer between the sections is a function of the number of turns, the coupling coefficients and the quality factors of the coils, thus quantifying the received power well.

4.3. One Section Peer-to-peer (Line of Sight)

The power relationship in a one-to-one transmitting system is of great interest as it applies to many applications which do not require range

extension. When $n = 0$ (reduced model) the peer-to-peer system has path loss equation:

$$\frac{P_R}{P_T} = \frac{Q_T \cdot Q_R N^2 \pi^2 k^2 (x)}{(2 + Q_T \cdot Q_R \cdot N^2 \pi^2 k^2 (x))} \tag{27}$$

i) When $Q_T \cdot Q_R \cdot N^2 \pi^2 k^2 (x) \gg 2$ the power equation approaches the value $P_R/P_T \approx 1$. This is a strong coupling case and the distance between the transmitter and receiver is close to zero, $d \to 0$. The received powers in most communication systems are usually not equal to the transmitted power due to losses in the channel and the transceiver circuitry.

ii) When

$$Q_T \cdot Q_R \cdot N^2 \pi^2 k^2 (x) = 2; \qquad P_R/P_T = 1/2 \tag{28}$$

We also have a relatively strong coupling case. This approximation promises that 50% the transmitted power can be delivered to the load. This level of efficiency is achievable with current inductive systems.

iii) When $Q_T \cdot Q_R \cdot N^2 \pi^2 k^2 (x) \ll 2$, or $k^2 (x)$ is small (weak coupling), a more practical situation, then

$$\frac{P_R}{P_T} \approx \frac{Q_T \cdot Q_R N^2 \pi^2 k^2 (x)}{2} \tag{29}$$

Even by using different assumptions, we arrive at a familiar expression. The reduced model and the AM models are equivalent (to within a constant multiplier). Thus the Agbinya-Masihpour model and Sun [2] model are identical and correctly model MI communications systems.

4.4. Multiple Sections Waveguide (Chain Network)

In this section N loop waveguide is investigated.

i) When the approximation $Q_T \cdot Q_R \cdot N^2 \pi^2 k^2 (x) \gg 2$ is used, the expression for the multi-section waveguide simplifies to:

$$\frac{P_R}{P_T} \approx \left(Q_T \cdot Q_R N^2 \pi^2 k^2 (x) \right)^n \left[\frac{j}{(Q_T \cdot Q_R N^2 \pi^2 k^2 (x))} \right]^{2n} \tag{30}$$

ii) However when $Q_T \cdot Q_R \cdot N^2 \pi^2 k^2(x) = 2$, the approximation gives:

$$\frac{P_R}{P_T} = \frac{2^n}{4} \left[\frac{j}{3} \right]^{2n} \tag{31}$$

For n sections, the communication distance $d = n \cdot x$, the link budget equation is

$$d = 10^{(P_T \, (\text{dBm}) - P_R \, (\text{dBm}) - 6 - 6.541n)} \tag{32}$$

iii) When $Q_T \cdot Q_R \cdot N^2 \pi^2 k^2 \, (x) \ll 2$ the power equation simplifies to

$$\frac{P_R}{P_T} \approx \text{Real} \left(\frac{1}{2} \left(Q_T \cdot Q_R N^2 \pi^2 k^2 \, (x) \right)^{n+1} e^{j\pi \cdot n} \right) \tag{33}$$

This expression is truly the $(n + 1)$ section power and the received power is always less than the transmitted power.

5. EXCITATION METHODS

Array excitation defines how the input signals are introduced to the transmitters to be coupled to the receivers. Four methods are proposed.

5.1. Array Edge Excitation

In the array edge excitation (AEE), the relay nodes are edge excited by lining up the transmitter directly opposite the relay node 1 as shown in Figure 3. The transmitter axis is at 90 degrees to the array axis. The transmitter coil has a radius of 6 mm and the receiver coils have identical radius of 3.5 mm with each one wound on a ferrite former. Array element n is inclined by an angle θ_n with respect to the
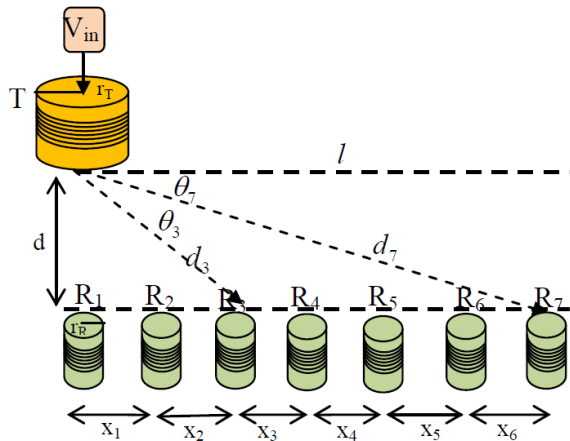
Figure 3. Array edge excited SIMO system.

transmitter and the length of the array is l. The diagonal distance linking the transmitter and receiver n is d_n and n is the node index. Generally

$$d_n^2 = d^2 + l_n^2; \quad l_n = \sum_{j=1}^{n-1} x_j. \tag{34}$$

In the following analysis, nearest neighbor coupling (NNC) concept in which node n is influenced by only nodes $(n-1)$ and $(n+1)$ and no other mutual induction from far away nodes is experienced is used. It is also extended to when more than one node on either side of a node influence it and their significances are quantified. The power received by a node n (section) without influence is given by the expression:

$$\frac{P_{Rn}}{P_T} \approx \frac{Q^2 N^2 \pi^2 k^2 (d_n) \cos^6 \theta_n}{2} \tag{35}$$

This power decays with the sixth power of the misalignment angle between a receiver and transmitter causing significant reduction in the received power and is a cause of reduced optimum power reception in MI systems. Figure 3 consists of seven receiving nodes and except for node $n = 1$, all the other nodes are misaligned by some angle from the transmitter. Using NNC, node 7 at the edge is influenced by node six only and its total power is:

$$\frac{P_{R7}}{P_T} \approx \frac{Q^2 N^2 \pi^2 k^2 (d_7) \cos^6 \theta_7}{2} + \frac{Q^2 N^2 \pi^2 k^2 (d_6) \cos^6 \theta_6}{2} \times \frac{Q^2 N^2 \pi^2 k^2 (x)}{2}$$
$$= \frac{Q^2 N^2 \pi^2}{2} \left(k^2 (x) \frac{Q^2 N^2 \pi^2 k^2 (d_6) \cos^6 \theta_6}{2} + k^2 (d_7) \cos^6 \theta_7 \right)$$
$$= \alpha \cdot \beta \cdot \left[k^2 (d_6) \cos^6 \theta_6 + \beta^{-1} k^2 (d_7) \cos^6 \theta_7 \right] \tag{36}$$

Similarly the power received by node 6 is

$$\frac{P_{R6}}{P_T} \approx \frac{Q^2 N^2 \pi^2 k^2 (d_6) \cos^6 \theta_6}{2} + \frac{Q^2 N^2 \pi^2 k^2 (d_7) \cos^6 \theta_7}{2} \times \frac{Q^2 N^2 \pi^2 k^2 (x)}{2}$$
$$+ \frac{Q^2 N^2 \pi^2 k^2 (d_5) \cos^6 \theta_5}{2} \times \frac{Q^2 N^2 \pi^2 k^2 (x)}{2}$$
$$= \alpha \cdot \beta \cdot \left[k^2 (d_5) \cos^6 \theta_5 + \beta^{-1} k^2 (d_6) \cos^6 \theta_6 + k^2 (d_7) \cos^6 \theta_7 \right] \tag{37}$$

where $\alpha = \frac{Q^2 N^2 \pi^2}{2}$ and $\beta = \frac{Q^2 N^2 \pi^2 k^2 (x)}{2}$. In general the receiver n power is:

$$P_{Rn} = \alpha\beta \cdot \left[k^2 (d_{n-1}) \cos^6 \theta_{n-1} + \beta^{-1} k^2 (d_n) \cos^6 \theta_n \right.$$
$$\left. + k^2 (d_{n+1}) \cos^6 \theta_{n+1} \right] \cdot P_T \tag{38}$$

In practice the coupling coefficients $k(x)$ are small values and the power received from the nearest neighbours is, therefore, small compared with the direct signal between the transmitter and a receiver. When $x_{n-1} \neq x_n \neq x_{n+1}$, and using α only the general equation may also be written as:

$$
\begin{aligned}
P_{Rn} = {} & \alpha^2 \cdot \left[k^2 \left(x_{n-1} \right) k^2 \left(d_{n-1} \right) \cos^6 \theta_{n-1} + \alpha^{-1} k^2 \left(d_n \right) \cos^6 \theta_n \right. \\
& \left. + k^2 \left(x_{n+1} \right) k^2 \left(d_{n+1} \right) \cos^6 \theta_{n+1} \right] \cdot P_T
\end{aligned}
\tag{39}
$$

Let N nodes on either side of the receiver have influence on its received power. For such a case the total received power at node n becomes:

$$
\begin{aligned}
P_{Rn} = {} & \sum_{j=0}^{N} \alpha^{j+1} \left[k^2 \left(d_{n-j} \right) \cdot \cos^6 \theta_{n-j} \prod_{i=0}^{j} k^2 (x_{n-i}) \right. \\
& \left. + k^2 (d_{n+j}) \cdot \cos^6 \theta_{n+j} \prod_{i=0}^{j} k^2 (x_{n+i}) \right] \cdot P_T \qquad k^2(x_n) = 1/2
\end{aligned}
\tag{40}
$$

When $k^2 \left(x_n \right) = 1/2$, the above equation is general for all n.

5.2. Array Centre Excitation

In array center excitation (ACE), the relay nodes are center excited and the transmitter is at a distance d directly opposite the relay node at the middle of the array as shown in Figure 4. The objective for the design is to achieve single input multiple output configuration.
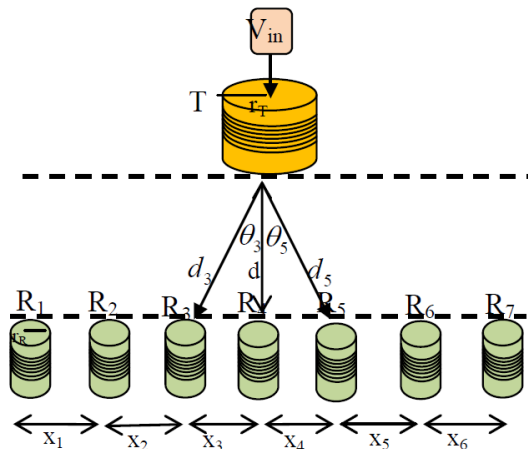
Figure 4. Array center excited SIMO system.

The power received by the receiver n with NNC consideration is given by the expression:

$$P_{Rn} = \alpha^2 \cdot \left[k^2 \left(x_{n-1} \right) k^2 \left(d_{n-1} \right) \cos^6 \theta_{n-1} \right.$$
$$\left. + k^2 \left(x_{n+1} \right) k^2 \left(d_{n+1} \right) \cos^6 \theta_{n+1} + \alpha^{-1} k^2 \left(d_n \right) \cos^6 \theta_n \right] \cdot P_T \quad (41)$$

In a symmetrical arrangement of the array elements with respect to the transmitter location, the following conditions hold for a receiver n: $\theta_{n-1} = \theta_{n+1}$; $x_{n-1} = x_{n+1}$ and $d_{n-1} = d_{n+1}$. Hence

$$P_{Rn} = \alpha^2 \cdot \left[2 k^2 \left(x_{n+1} \right) k^2 \left(d_{n+1} \right) \cos^6 \theta_{n+1} + \alpha^{-1} k^2 \left(d_n \right) \cos^6 \theta_n \right] \cdot P_T \quad (42)$$

For multi-neighbour interaction by N nodes on either side, the received power by node n is:

$$P_{Rn} = \alpha \cdot k^2 \left(d_n \right) \cdot \cos^6 \theta_n$$
$$+ 2 \sum_{j=0}^{N} \alpha^{j+1} \left[k^2 \left(d_{n+j} \right) \cdot \cos^6 \theta_{n+j} \prod_{i=0}^{j} k^2 \left(x_{n+i} \right) \right] \cdot P_T \quad (43)$$

The gain obtained by ACE is significant if the nodes cooperate and reinforce each other. When the array is centre excited and the nodes are not symmetrically placed with respect to the transmitter, the received power is:

$$P_{Rn} = \alpha \cdot k^2 \left(d_n \right) \cdot \cos^6 \theta_n + \sum_{j=0}^{N} \alpha^{j+1} \left[k^2 \left(d_{n+j} \right) \right.$$
$$\left. \cdot \cos^6 \theta_{n+j} \prod_{i=0}^{j} k^2 \left(x_{n+i} \right) + k^2 \left(d_{n-j} \right) \cdot \cos^6 \theta_{n-j} \prod_{i=0}^{j} k^2 \left(x_{n-i} \right) \right] \cdot P_T \quad (44)$$

When the array is not perpendicular to the excitation source, Equation (44) holds. However, the values of d_n which reflect the lateral shift of the array with respect to the excitation should be used.

5.3. Collinear Array Excitation

In the collinear array excitation (CAE), the transmitter axis is collinear with the array axis and the nodes form a linear chain network. All the array elements including the transmitter are separated from each other by distance x. A previous node serves as the exciter for its neighbor and the power received by node n is obtained recursively as

$$P_{R1} \approx \frac{Q^2 N^2 \pi^2 k^2 \left(x \right)}{2} P_T;$$
$$P_{R2} \approx \frac{Q^2 N^2 \pi^2 k^2 \left(x \right)}{2} P_{R1} = \left(\frac{Q^2 N^2 \pi^2 k^2 \left(x \right)}{2} \right)^2 P_T \quad (45)$$

The power received by node n is thus given as

$$P_{Rn} \approx \frac{Q^2 N^2 \pi^2 k^2 (x)}{2} P_{R(n-1)} = \left(\frac{Q^2 N^2 \pi^2 k^2 (x)}{2} \right)^n P_T;$$

$$P_{Rn} \approx \left(\frac{1}{2} \right)^{n+1} \left(Q^2 N^2 \pi^2 k^2 (x) \right)^{n+1} P_T \tag{46}$$

The last equation is for $(n+1)$ sections. The power expression is similar to the MI waveguide and has no phase term as in the original MI waveguide equation. These equations show that CAE power transfer capability is very poor for nodes which are not near the transmitter because of being shielded by other nodes from the effects of the receiver leading to increasingly weak coupling of flux the farther away the node is from the transmitter.

5.4. Multiple Array Excitation

In the multiple array excitation (MAE) several arrays are used concurrently as in Figure 5 and each array is excited separately. The multiple arrays open up several options for array deployment. There may be only an excitation, or each array may be excited or only a subset of the array is excited.
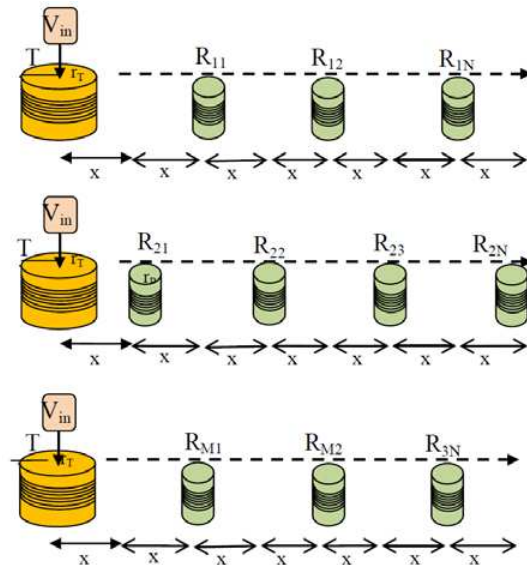
Figure 5. Multiple array excitation (MAE).

Assume that the nodes in each array are arranged in a regular manner, equidistant (may not be so all the time) from each other and excited as in CAE. The arrays are of the same length. We also assume that the distance between the arrays is large enough to prevent neighbouring arrays from interfering with each other. The arrays are of infinite length with no reflections. In a multi-array system, the receiver n taps its signals from each array at location n.

Thus the receiver is separate from the system of arrays. The received signal by receiver n when the transmitter excitations are equal is given by the expression:

$$P_n = \sum_{j=1}^{M} P_{Rj} = P_T \sum_{j=1}^{M} \left(\frac{1}{2}\right)^{nj} \left(Q^2 N^2 \pi^2 k^2 (d_{nj})\right)^{nj} \cos^6 (\theta_{nj}) \quad (47)$$

where M is the number of arrays with index j and n is the node location inside each array where flux is tapped into the receiver. This relay system consists of M transmitters each serving n nodes (a total of $M \times N$ nodes). A receiver listens to M main sources, one from each array provided the transmitters are in its neighbourhood. The distance between array elements is $2x$. The MAE system is suitable for multi-channel MI communication and may require coding of channel signals to enable easy separation at the receiver. It may also use OFDM system.

6. SIMULATION AND EXPERIMENTAL RESULTS

We conducted various experiments with both hardware and software when the receivers are located within the near field region of the transmitter. Multiple relay nodes were designed and arranged in a chain network. They were deployed on a wooden holder and each node is a stand alone with no physical connections to its neighbours. One transmitter was also designed using a 151 μH inductor connected to a 39 μF capacitor and excited with an input at 2.65 MHz frequency. Figure 3 shows the hardware set up for the experiments. Using AEE architecture the received power profile was measured with a software oscilloscope attached to a laptop. An exponentially decaying power profile with a maximum value at the coil at the array edge opposite the transmitter was observed. When the transmitter input voltage is 30 mV and the receiver node at 2.3 cm from it, the received voltage is 520 mV, a gain of 17.3 at bore site (Figure 6). The receiver array was moved to 5 cm from the transmitter still within the near-field region of the transmitter. The received voltage at bore sight was measured to be 46 mV, a voltage gain of 1.53. The receiver array was moved
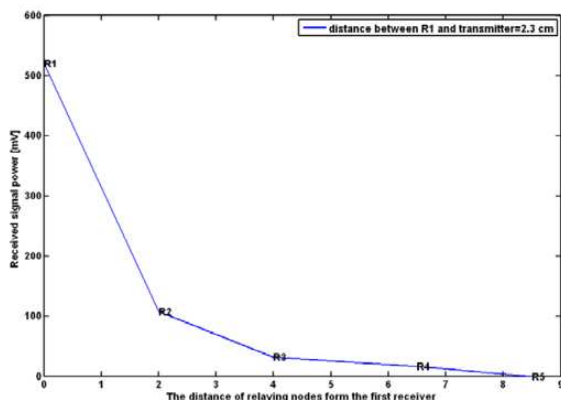
Figure 6. Received power by nodes 1 to 5 in AEE.
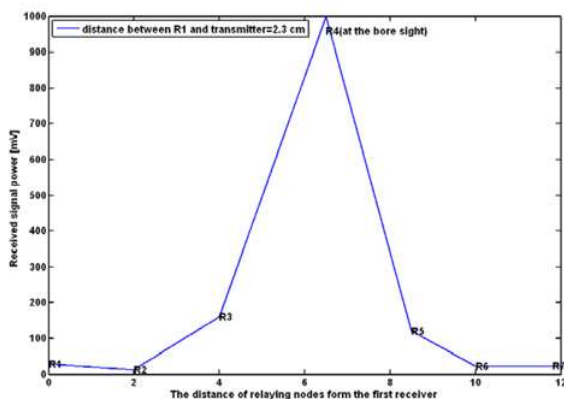
Figure 7. Array power gain profile.

further to 7 cm from the transmitter. The received voltage at bore sight is 27 mV, a gain of 0.9. Thus the received power decreases very fast as the receiver is moved away from the transmitter. In Figure 7, the receiver arrays were located at 2.3 cm, 5.0 cm and 7 cm from the transmitter. Very high induced power was recorded at distances very close to the transmitter and decrease rapidly as the array is moved away to 5 cm and then to 7 cm.

Despite the apparent gains provided by the ACE arrangement the intention of this section is to show that significant gains are obtained using NNC and the advantages in using multiple neighbour interaction become more and more insignificant the further away the nodes are

from the receiver. This is due to shielding by other nodes on both sides and also highly reduced mutual inductance between the nodes. For example, let $d = 5$ m; $x_j = 10$ m; $r_T = 10$ cm and $r_R = 5$ cm. Then

$$d_1^2 = d^2 + x_1^2 = 25 \cdot 10^4 + 10^6 \text{ cm}^2 = 125 \cdot 10^4 \text{ cm}^2;$$

$$\cos\theta_1 = \frac{5}{\sqrt{125}}; \quad \cos^6\theta_1 = \left(\frac{1}{125}\right)$$

$$k^2(d) \approx \frac{r_T^3 r_R^3}{d^6} = \frac{1}{(125)^2 \cdot 10^6};$$

$$k^2(d_{n+1}) \approx \frac{r_T^3 r_R^3}{d_1^6} = \frac{10^3 \cdot 5^3}{\left[100\left(\sqrt{125}\right)\right]^6} = \frac{1}{10^9 (125)^2};$$

$$k^2(x_{n+1}) \approx \frac{r_T^3 r_R^3}{x_{n+1}^6} = \frac{10^3 \cdot 10^3}{(1000)^6} = \frac{1}{10^{12}}$$

Let the transmitter and receiver coils have $Q = 100$ and turns $N = 10$, the power received from first neighbour is about

$$\begin{aligned}
\Delta P &= \frac{Q^2 N^2 \pi^2 k^2(d_{n+1}) \, k^2(x_{n+1}) \cdot \cos^6\theta_1}{P_n} \\
&= \frac{\left(Q^2 N^2 \pi^2\right)^2 k^2(d_{n+1}) \, k^2(x_{n+1}) \cos^6\theta_1}{Q^2 N^2 \pi^2 k^2(d)} \\
&= \frac{10^6 \pi^2}{10^9 (125)^2} \frac{1}{10^{12}} \times 10^{12} (125)^2 \cdot \frac{1}{125} = \frac{\pi^2}{(125) 10^3} \approx \frac{1}{125}\% \quad (48)
\end{aligned}$$

Thus the power contributed by a nearest neighbour in this case is about $(1/125)\%$ of the direct power received by node n from the transmitter. The two nearest neighbours contribute less than $(2/125)\%$ extra power. Therefore, the effects of remote neighbours are mostly insignificant. Hence we can safely ignore the influences of neighbouring nodes beyond the first one on both sides. Nearest neighbours will have more influence if coils of large Q and with more turns are deployed as neighbours. The received power profile with ACE is parabolic with peak centered at the middle coil. With a transmitter input voltage of 30 mV and receiver array located at 2.3 cm from it, the highest received voltage is 1000 mV (1 volt!), an impressive voltage gain of 33.3 at bore site (Figure 7). The receiver array was moved to again to 5 cm from the transmitter, and the received voltage at bore sight is 120 mV, a gain of only 4. The receiver array was moved once more further to 7 cm from the transmitter, and the received voltage at bore site is 40 mV, a gain of 1.33. In general, despite the 6th power of distance power decrease for the transceivers, the received power at a point can be increased by using an array of receivers.

7. CONCLUSIONS

We have provided a detailed analysis of magneto-inductive channels and link budgets showing that nearest neighbour interaction plays a part in the received signals in waveguide systems. In the relay systems, we have also shown that only first nearest neighbours on either sides of the node have the most significant effect on it. This influence can be beneficial. Various forms of array excitations are used showing that array centre excitation is optimum in terms of all the arrays studied in the paper. Theoretical analyses were justified with realistic experimental demonstration.

REFERENCES

1. Agbinya, J. I., *Principles of Inductive Near Field Communications for Internet of Things*, River Publishers, Denmark, 2011, ISBN: 978-87-92329-52-3.

2. Sun, Z. and I. F. Akyildiz, "Underground wireless communications using magnetic induction," *Proc. IEEE ICC*, 1–5, 2009.

3. Akyildiz, I. F. and E. P. Stuntebeck, "Wireless underground sensor networks: Research challenges," *Ad Hoc Networks Journal*, Elsevier, Vol. 4, 669–686, Jul. 2006.

4. Li, L., M. C. Vuran, and I. F. Akyildiz, "Characteristics of underground channel for wireless underground sensor network," *Proc. Med-Hoc Net*, Corfu, Greece, Jun. 2007.

5. Sojdehei, J. J., P. N. Wrathall, and D. F. Dinn, "Magneto-inductive (MI) communications," *Proc. MTS/IEEE Conference and Exhibition (OCEANS)*, 513–519, Nov. 2001.

6. Agbinya, J. I., N. Selvaraj, A. Ollett, S. Ibos, Y. Ooi-Sanchez, M. Brennan, and Z. Chaczko, "Characteristics of the magnetic bubble 'Cone of Silence' in near-field magnetic induction communications terminals," *Journal of Battlefield Technology*, Vol. 13 No. 1, 21–25, Mar. 2010.

7. FreeLinc, FreeLinc Products, accessed Mar. 3, 2009, http://www.freelinc.com/products/.

8. Sauer, C., M. Stanacevic, G. Cauwenberghs, and N. Thakor, "Power harvesting and telemetry in CMOS for implanted devices," *IEEE Trans. on Circuits and Systems — I: Regular Papers*, Vol. 52, No. 12, 2605–2613, Dec. 2005.

9. Galbraith, D. C., M. Soma, and R. L. White, "A wide-band efficient inductive transdermal power and data link with coupling

insensitive gain," *IEEE Transactions on Biomedical Engineering*, Vol. 34, No. 4, 265–275, Apr. 1987

10. Jiang, H. C. and Y. E. Wang, "Capacity performance of an inductively coupled near field communication system," *Proc. IEEE International Symposium of Antenna and Propagation Society*, 1–4, Jul. 5–11, 2008.

11. Evans-Pughe, C., "Close encounters of the magnetic kind," *IEE Review*, 38–42, May 2005.

12. Bansal, R., "Near field magnetic communications," *IEEE Antennas and Propagation Magazine*, Vol. 46, No. 2, 114–115, Apr. 2004.

13. Lee, K. and D.-H. Cho, "Adaptive tuning method for maximizing capacity in magnetic induction communication," *Proc. IEEE ICC*, 4310–4313, 2012.

14. Akyildiz, I. F., Z. Sun, and M. C. Vura, "Signal propagation techniques for wireless underground communication networks," *Physical Communication 2*, Elsevier, 167–183, 2009

15. Syms, R. R. A., E. Shamonina, and L. Solymar, "Magneto-inductive waveguide devices," *Proceedings of IEE Microwaves, Antenna and Propagation*, Vol. 153, No. 2, 111–121, 2006.

16. Shamonina, E., V. A. Kalinin, K. H. Ringhofer, and L. Solymar, "Magneto-inductive waveguide," *Electron. Letters*, Vol. 38, No. 8, 371–373, Apr. 11, 2002.

17. Kalinin, V. A., K. H. Ringhofer, and L. Solymar, "Magneto-inductive waves in one, two and three dimensions," *Journal of Applied Physics*, Vol. 92, No. 10, 6252–6261, 2002.

18. Kopparthi, S., "Remote power delivery and signal amplification for MEMS applications," MSc. Thesis, Andhra University, India, Dec. 2003.

19. Jiang, B., J. R. Smith, M. Philipose, S. Roy, K. Sundara-Rajan, and A. V. Mamishev, "Energy scavenging for inductively coupled passive RFID systems," *Instrumentation and Measurement Technology Conference*, Ottawa, Canada, May 17–19, 2005.

20. Jiang, B., J. R. Smith, M. Philipose, S. Roy, K. Sundara-Rajan, and A. V. Mamishev, "Energy scavenging for inductively coupled passive RFID systems," *IEEE Trans. on Instrumentation and Measurement*, Vol. 56, No. 1, 118–125, Feb. 2007

21. Syms, R. R. A., O. Sydoruk, E. Shamonina, and L. Solymar, "Higher order interactions in magneto-inductive waveguides," *Metamaterials*, Vol. 1, 44–51, 2007.

22. Grace, R. J., "Bio magnetic energy in pain relief and healing,"

Proc. 2nd International Conference on Bioelectromagnetism, 143–144, Melbourne, Australia, Feb. 1998.

23. Agbinya J. I. and M. Masihpour, "Power equations and capacity performance of magnetic induction communication systems," *Wireless Personal Communications*, Vol. 64, No. 4, 831–845, Springer, Jun. 2012.

24. Agbinya, J. I. and M. Masihpour, "Near-field magnetic induction communication link budget: Agbinya-masihpour model," *Proc. of IB2Com*, Malaga, Spain, Dec. 15–18, 2010.

25. Fatiha, E. H., G. Marjorie, S. Protat, and O. Picon, "Link budget of magnetic antennas for ingestible capsule at 40 MHz," *Progress In Electromagnetic Research*, Vol. 134, 111–131, 2013.

26. Lee, K. and D.-H. Cho, "Adaptive tuning method for maximizing capacity in magnetic induction communication," *Proc. IEEE ICC*, 4310–4314, 2012.

27. Agbinya, J. I., "A magneto-inductive link budget for wireless power transfer and inductive communication systems," *Progress In Electromagnetics Research C*, Vol. 37, 15–28, 2013.